IL NUOVO CIMENTO Vol. 25 C, N. 5-6 Settembre-Dicembre 2002

The investigation of the physical conditions in the flare H_α loop by the semiempirical simulations(*)

S. N. Chornogor and K. V. Alikaeva
Main Astronomical Observatory of NASU - 03680, Zabolotnoho Str. 27, Kyiv, Ukraine

(ricevuto il 10 Giugno 2002; approvato il 24 Settembre 2002)

Summary. — Semiempirical models of the photospheric part of H_α flare loop are constructed as stratifications with optical depth of thermodynamic and magnetic parameters and the line-of-sight (LOS) velocities. The models obtained reveal the presence of some inhomogeneous layers. These inhomogeneities penetrate in the photosphere down to its base during the impulsive phase of the flare and the disturbances dissipate with time. The character of such photospheric models can be explained by the propagation of a wave packet from the region of the magnetic reconnection in the upper atmosphere.

PACS 96.60.Mz – Photosphere, granulation.
PACS 92.60.Ek – Convection, turbulence, and diffusion.
PACS 01.30.Cc – Conference proceedings.

1. – Introduction

The observational data on solar flares stored during the last decades show that all the layers of the solar atmosphere take part in the flare process. This statement must be taken into account when real hydrodynamical models are built. Unfortunately, the theoretical models of the hydrodynamical response ignore the deep photospheric layers of the flare atmosphere [1, 2].

During the last years a number of papers appeared [3-6] discussing the importance of the processes in the photosphere at the early stage of a flare or before it. These processes were considered as the origin of the ascent of the magnetic loops and then their fast reconnection with a large-scale field in the corona. This leads to eruptive release of the flare energy.

The semiempirical models are scanty and most of them describe the state of the chromosphere and high levels of the photosphere [7-9], as a rule. In addition, these models

(*) Paper presented at the International Meeting on THEMIS and the New Frontiers of Solar Atmosphere Dynamics, Rome, Italy, March 19-21, 2001.

Table I.

λ (nm)	Element	$h\nu_{\rm low}$ (eV)	$g_{\rm eff}$	$h_{\rm d}$ (km)
654.625	Fe I	2.75	0.83	435
655.423	Ti I	1.44	1.08t	238
655.547	Si I	5.94	1.00	209
655.607	Ti I	1.45	1.25t	246
655.680	Fe I	4.77	0.50	203
657.278	Ca I	0.00	1.50t	274
657.423	Fe I	0.99	1.25	287

do not contain information on some flare details such as flare loops or ribbons. The semiempirical modeling based on the analysis of Fraunhofer spectra of flare regions give the opportunity to investigate the flare deep photospheric layers of flare atmosphere [10].

2. – Observations

Here we study velocity field and thermodynamical state of matter at the photospheric levels of different parts of the flare H_α loop of the faint solar flare sf/c5 on 2 August 1990 (flare onset: 05.45 UT, maximum: 05.49 UT, end: 06.03 UT). We use the photographic spectral observations at the Horizontal Solar Telescope (ATsU-26) at the Peak Terskol ($h = 3200$ m) of the Main Astronomical Observatory of the National Academy of Sciences of Ukraine. These observations allowed us determine the physical conditions in different parts of the flare H_α loops. The observational period included the flare H_α maximum and a gradual phase. The H_α images of the active region were recorded with a TV-camera. The flare was seen as several H_α loops near the spot-leader. The spectrograph slit crossed the east branches of two loops including the regions near their tops and bases.

The photometry was made with an automatic digital two-coordinate microphotome-

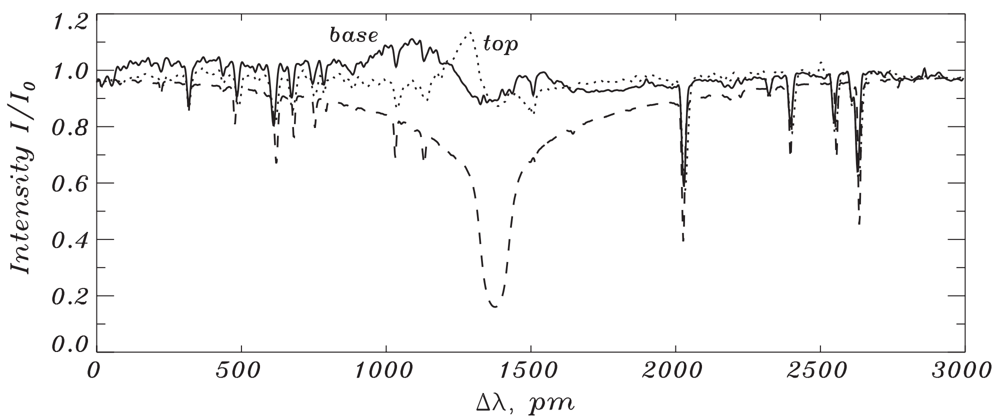

Fig. 1. – H_α profiles. Dotted line: the non–self-reversed profile corresponding to the loop top. Solid line: the profile with a self-reversal corresponding to the flare base. Dashed line: the profile formed at the quiet atmosphere.

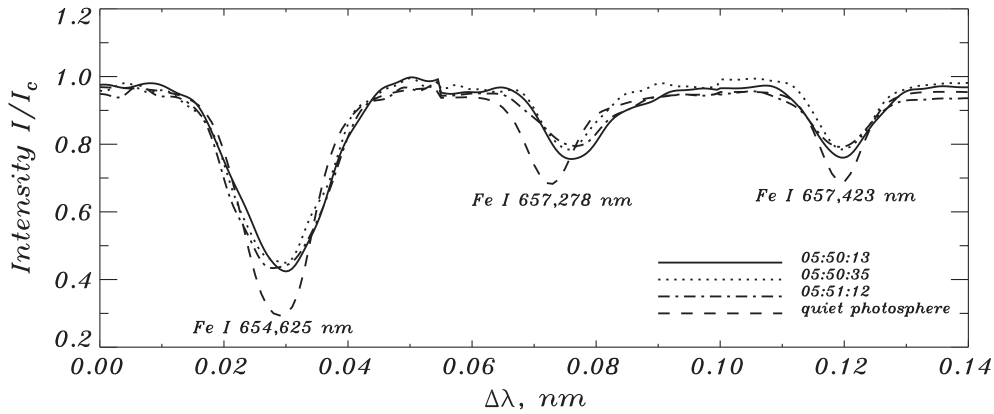

Fig. 2. – The observed profiles of some Fraunhofer lines at the flare loop base; the profiles in the quiet photosphere are shown by the dashed line.

ter. The spatial resolution along the slit was 2.″3 and spectral resolution was 1 pm for H_α and 0.5 pm for Fraunhofer lines. The H_α profiles for different moments reveal variations of shape along the loop (fig. 1). Flare knots with emission in the H_α core are clearly seen close to the moustache emission knots. The H_α profiles with core emission, corresponding geometrically to the loop tops, are transformed into profiles with central absorption near the loop bases.

Table I contains a list of the Fraunhofer lines forming in the high and middle photosphere ($200 < h < 450$ km) used for the determination of the LOS velocities and simulations. The heights of line center formation ($h_{\rm d}$) in the undisturbed photosphere ($\cos\theta = 0.512$) were calculated using the SPANSAT program [11]. These heights may differ from the real heights in the flare because of the distinctions between the flare and undisturbed atmosphere models.

The observed profiles were corrected for the instrumental profile of the fourth-order spectrum of the spectrograph of ATsU-26 solar telescope. The largest changes were detected in the Fe I λ 654.625 nm line which is formed near the temperature minimum region in the quiet photosphere. This line becomes substantially weaker (shallower by 20%) and wider. Similar changes occur in other lines as well (fig. 2). The largest variations were noticed one minute after the H_α-maximum of the flare. These peculiarities of spectral line profiles can be described by the semiempirical models constructed in this study.

3. – Semiempirical photospheric simulations

We calculated the semiempirical models of the photospheric part of the flare loop as stratification of temperature (T), total hydrogen number density ($n_{\rm H}$), electron number density ($n_{\rm e}$), LOS velocities (v) and longitudinal magnetic-field intensity ($H_{||}$) with optical depth τ_5. The theoretical line profiles were calculated using an LTE computational code. The code allows us to reveal the thermodynamic and magnetic properties of the loop details by fitting the shape of the observed line profiles by trial and error method. Besides, the corrections to Saha and Bolzman equations are done for the uppermost photospheric layers. The choice of the models is not restricted by the requirement of

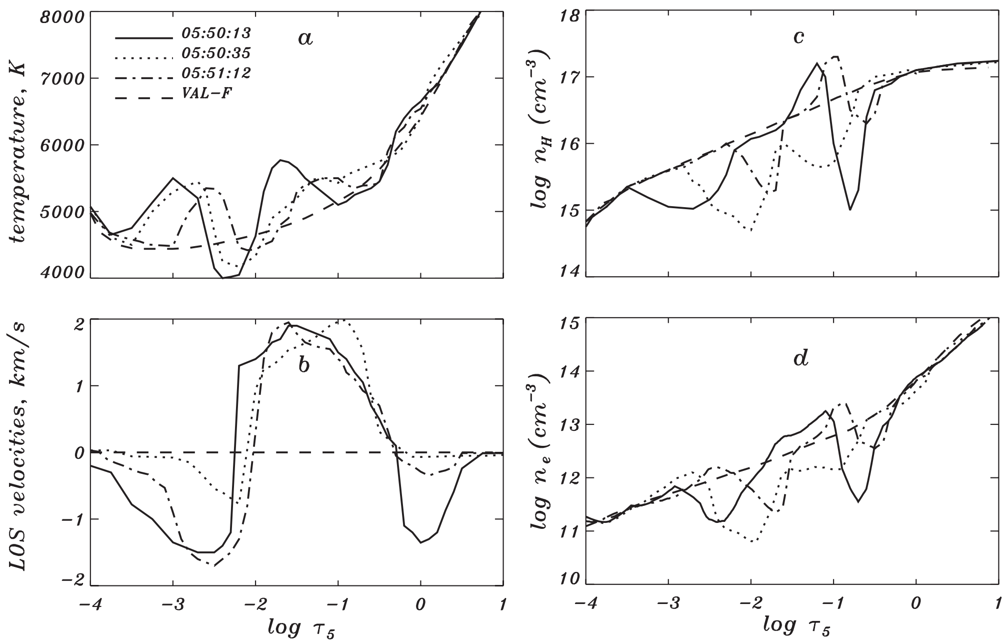

Fig. 3. – The stratifications of temperature (a), LOS velocities (b), total hydrogen number density (c) and electron number density (d) with optical depth τ_5 during the impulsive phase of the flare at the loop base; the VAL-F model is shown by the dashed curve.

the hydrostatic equilibrium because this condition is possibly not fulfilled in an active atmosphere. The line profiles were calculated for Fe and Si atom models comprising 15 levels and continuum and Ca and Ti atom models with 8 levels and continuum. The continuous absorption coefficient used accounts for the absorption by the atoms and negative ions of hydrogen, C I, Si I, Mg I, Al I, and Fe I atoms as well as scattering by free electrons and hydrogen atoms.

The code gives the possibility to calculate profiles of magnetosensitive lines for the longitudinal or transverse magnetic-field components taken into account through the Unno equations for the Stokes parameters modified for observations without polarizing optics.

The abundances of elements, oscillator strengths, and Van-der-Waals and Stark constants are found by fitting the quiet-photosphere model VAL-C to the observed line profiles outside the active region. An additional restriction for the selection of models concerns the continuum intensity level. It should correspond to the observed intensity at the given cos θ within 1%. The program we used for line profile calculations is described in [12]. The fit of models to observations was performed within the observational error limits: $\Delta d_0 < 1$ % for central intensities and $\Delta\lambda_{1/2} < 1$ pm for half-widths.

Figure 3 demonstrates the stratifications of temperature (T), total hydrogen number density ($n_{\rm H}$), electron number density ($n_{\rm e}$) and LOS velocities (v) with optical depth during the impulsive phase of the flare at the loop base obtained from the procedure. The VAL-F model [13] of bright plage is shown for comparison (dashed curve).

The models reveal the presence of inhomogeneous layers in the upper and middle photosphere. The temperature excess relative to VAL-F model is about 1000 K at the

H_α flare maximum, and it shows the tendency to decrease during the impulsive phase (fig. 3a). The LOS velocities vary from -1.8 km s^{-1} in the highest and deepest layers up to 2 km s^{-1} in the middle photosphere (fig. 3b). Thus, descending motions are predominant in the layers where the cores of Fraunhofer lines are formed. This causes the red shifts of the lines. As can be seen from fig. 3c, the stratifications of the total hydrogen number density $n_{\rm H}$ show layers of both higher and lower density relative to VAL-F. The density variations may be as much as two orders of magnitude. The stratifications of the electron number density $n_{\rm e}$ show similar tendency (fig. 3d). The magnetic-field strength was dose to 400 G in the deep photosphere and did not exceed 200 G in the upper and middle photosphere.

These flaky photospheric models are similar to the ones obtained by flare modeling from emission lines of neutral and ionized iron [8] and the Balmer profiles of moustaches [14]. In both cases the profiles peculiarities may be explained if the observed profiles are partially formed in discrete hot and dense atmospheric layers located at different heights. According to the opinion of the author of [14] there is a shock wave propagating in a flare kernel.

Another property of these models is a gradual displacement of the inhomogeneities to lower layers. This testifies to a disturbance which penetrates into the photosphere from above.

The geometrical heights of these inhomogeneities were determined from the condition of gas pressure balance inside and outside the flare:

$$[H^2/8\pi + P_{\rm g}]^{\rm flare} = P_{\rm g}^{\rm out}.$$

It was found the height difference between temperature peaks in high and middle photosphere varies from 300 km to 200 km during the impulsive phase. Besides, we found that the layers with temperature and density excesses move deep down with mean velocities of 2.37–3.64 km s^{-1} .

The simulation results may be explained as a propagation of a wave packet from the site of magnetic reconnection in the upper atmosphere. The velocities of the shock and acoustic waves were estimated using the models. They proved to be somewhat larger than those stated above. The nature of these waves is unknown yet. Thus, we may state that the disturbances penetrate to the low photosphere and dissipate there.

4. – Conclusions

The hydrodynamical flare models predict the formation of the condensation in the impulsive phase moving from the corona to the chromosphere and dissipating at the temperature minimum region [1, 15, 2]. Fisher, Canfield and McClymont [1] associate this condensation with a shock wave.

In our case the results we got are as following:

1) a common feature of semiempirical photospheric models is the presence of some inhomogeneous layers in the stratifications of temperature and density. These inhomogeneities are relatively thin heated layers. The stratifications of $n_{\rm H}$ and $n_{\rm e}$ show layers of both higher and lower density.

2) The temperature excess relative to VAL-F model is of about 1000 K. The total hydrogen number density $n_{\rm H}$ and electron number density $n_{\rm e}$ variations can be as much as two orders of magnitude.

3) The temperature in the inhomogeneous layer decreases in the lower photosphere during the impulsive phase.

4) At the impulsive phase the disturbances penetrate to the low photosphere with velocities of 2.37–3.64 km s^{-1} and dissipate there.

The character of the semiempirical models of the photospheric part of the flare loop may be interpreted as a propagation of a wave packet from the region of magnetic reconnection in the upper atmosphere. The nature of these waves is unknown yet.

REFERENCES

[1] Fisher G. H., Canfield R. C. and McClymont A. N., *Astrophys. J.*, **289** (1985) 414.
[2] Somov V. B., Spector A. R. and Syrovatsky S. I., *The Flare Processes in Plasma, Transactions of Physical Institute*, **110** (1979) 73 (in Russian).
[3] Litvinenko Yu. E., *Astrophys. J.*, **515** (1999) 435.
[4] Ruderman M. S., Goosens M., Ballester J. L. and Oliver R., *Astron. Astrophys.*, **328** (1997) 361.
[5] Titov V. S. and Demoulin P., *Astron. Astrophys.*, **351** (1999) 707.
[6] Zhang H. Q., Sakurai T., Shibata K. *et al.*, *Astron. Astrophys.*, **357** (2000) 725.
[7] Alikaeva K. V., Baranovsky E. A. and Polupan P. N., *Solar Maximum Analysis*, in *Proceedings of the International Workshop, Irkutsk, 1988*, pp. 84-87.
[8] Baranovsky E. A. and Kurochka E. V., *Solnech. Dannye*, **10** (1989) 98 (in Russian).
[9] Gan W. Q., Rieger E. and Fang C., *Astrophys. J.*, **416** (1993) 886.
[10] Alikaeva K. V., Baranovsky E. A. and Kondrashova N. N., *Kinemat. and Phys. Celest. Bodies*, **11**, No. 2 (1994) 7.
[11] Gadun A. S. and Sheminova V. A., preprint Theor. Phys. Inst., **ITF-88-87R** (1988) (in Russian).
[12] Baranovsky E. A., *Contrib. Astron. Obs. Skalnate Pleso*, **23** (1993) 107.
[13] Vernazza J. E., Avrett E. H. and Loeser R., *Astrophys. J. Suppl. Ser.*, **45** (1981) 635.
[14] Kitai R., *Solar Phys.*, **87** (1983) 135.
[15] Nagai F. and Emslie A. G., *Astrophys. J.*, **279** (1984) 896.